THE FLORIDA STATE UNIVERSITY
COLLEGE OF ARTS AND SCIENCES

THE SEARCH FOR LARGE EXTRA DIMENSIONS VIA SINGLE PHOTON PLUS MISSING ENERGY FINAL STATES AT $\sqrt{s} = 1.96$ TeV

By
ALICIA GOMEZ

A Thesis submitted to the
Department of Physics
in partial fulfillment of the requirements for graduation with
Honors in the Major

Degree Awarded:
Spring, 2013

The members of the Defense Committee approve the thesis of Alicia K. Gomez defended on April 17, 2013.

_____

Dr. Todd Adams
Thesis Director

_____

Dr. Brian Ewald
Outside Committee Member

_____

Dr. Horst Wahl
Committee Member

There is a hierarchy problem present in the standard model of particle physics; the force of gravity is many magnitudes weaker than the other fundamental forces. The ADD model (Arkani-Hamad, Dimopoulos, Dvali) proposes a solution to this hierarchy problem though the introduction of large extra spatial dimensions. Using 7.3 fb^{-1} of data from the D0 detector at Fermi National Accelerator Laboratory, we analyze proton-antiproton collisions at $\sqrt{s} = 1.96$ TeV which result in one photon plus missing transverse energy, where this missing transverse energy is associated with a graviton traveling into another dimension. We set limits on the value of the fundamental Planck scale M_D from 1026 GeV to 868 GeV for two to eight extra spatial dimensions. This is a work in progress, and has not been approved by the D0 collaboration.

Contents

Part I
Introduction

1 Motivation

There are four fundamental forces in nature. They are the strong, weak, electromagnetic, and gravitational forces. These forces are not equal in strength. If the strength of the strong force is equal to 1, then the electromagnetic force is equal to 10^{-2}, the weak force is 10^{-6}, and the gravitational force is 10^{-39}. The large difference between the strengths of the gravitational force and the other fundamental forces is called the hierarchy problem.

A more formal way of looking at this hierarchy problem is to say that the electroweak scale is many magnitudes larger than the Planck scale. The electroweak scale is on the order of 10^3 GeV, while the Planck scale is on the order of 10^{18} GeV [1].

This leads to the question: why is the gravitational force so small compared to the other fundamental forces (or why is the ratio between the Planck scale and the electroweak scale so large)? This is the question we are trying to help answer in this analysis.

2 The ADD model

Nima Arkani-Hamad, Savas Dimopoulos, and Gia Dvali (ADD) proposed, in 1998, a solution to the hierarchy problem through the introduction of large (compared to the weak scale) extra spatial dimensions (LEDs). They theorized that the weakness of gravity was due to the fact that gravitons are able to transverse these extra dimensions, while standard model particles are confined to the three spatial dimensional universe we are familiar with. According to the ADD model, the fundamental scale is the electroweak scale. Therefore, the electroweak scale sets the scale of strength of the other forces, including that of gravity [1].

The ADD model presents a relation between the size of the extra dimension(s) $\{R\}$, the number of extra dimensions $\{n\}$, the effective Planck scale in 4 dimensional spacetime $\{M_{PL}\}$, and the fundamental Planck scale in the (n+4) dimensional spacetime $\{M_D\}$ [1]. Specifically,

$$M_{PL}^2 = 8\pi M_D^{n+2} R^n \tag{2.1}$$

Our goal is to set lower limits on allowed values of this fundamental Planck scale, M_D and thereby examine the number of extra dimensions that are (or are not) possible. The data used in this analysis is from the D0 detector at Fermi National Accelerator Laboratory. This particle accelerator is located in Batavia, Illinois. It collided protons and antiprotons at a center of mass energy, $\sqrt{s}$, of 1.96 TeV and recorded data on the products of this interaction. The specific reaction we analyzed, our signal, is one that results in a single photon and missing transverse energy (MET) (see Figure 2.1). Specifically,

$$p + \bar{p} \rightarrow \gamma + G_{KK} + X \tag{2.2}$$

In this reaction, the Kaluza-Klein Graviton (G_{KK}) is left undetected, and is associated with the missing transverse energy. Due to energy conservation, the energy before the collision in the transverse plane should be equal to the energy after the collision in the transverse plane. The detector can not detect all of the energy/particles that are produced, and this deficit of energy is labeled missing transverse energy.

3 Pertinent Detector Information

The D0 detector was used to measure data from proton-antiproton collisions that occurred at the Tevatron collider at Fermi National Accelerator Laboratory in Batavia, Illinois. The Tevatron collider was four miles in circumference and collided protons and antiprotons at a center of mass energy of 1.96 TeV. The Tevatron used a series accelerators to increase the

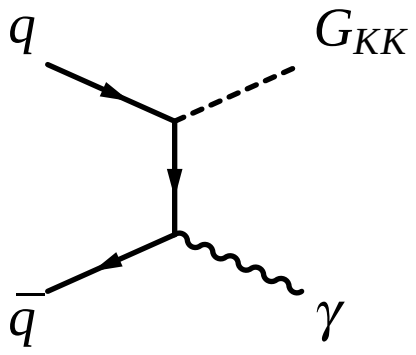

Figure 2.1: Feynman diagram of $p + \bar{p} \rightarrow \gamma + G_{KK} + X$. It is the quarks in the protons that are interacting.

velocity of a particle to 99.999954% the speed of light before they collided at the center of the two particle detectors located on site, at two straight sections of the collider, namely D0 and CDF [2].

The D0 detector is comprised of many different layers designed to make specific types of energy measurements to help identify the particles that arise from the proton-antiproton collisions. The two sections of the D0 detector that are pertinent to this analysis are the central preshower detector (CPS) and the electromagnetic (EM) calorimeter. The CPS is located in front of the calorimetry system and behind the 2 Tesla solenoid magnet (see Figure 3.1b). It is comprised of three layers of scintillating strips. This allows for precision measurements of the location of electromagnetic showers. The liquid-argon-uranium calorimeter has two main parts: the EM calorimeter and the hadronic calorimeter. The EM calorimeter is located before the hadronic calorimeter, closer to the beam tube. When an electromagnetic object transverses both the CPS and EM calorimeter, it deposits energy in these detector regions. This data is then reconstructed to determine what type of EM object was detected [3].

The D0 detector collected data over various Run periods. This analysis looks specifically at the RunII dataset. The RunII dataset is further divided into five different run periods. We analyze data from the RunIIa, RunIIb1, RunIIb2, and RunIIb3 (due to time constraints, RunIIb4 has not been fully analyzed and therefore temporarily omitted from this analysis).

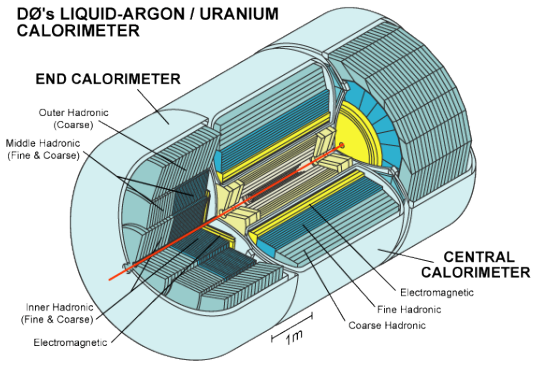

(a) Calorimetry region of the D0 detector[4].

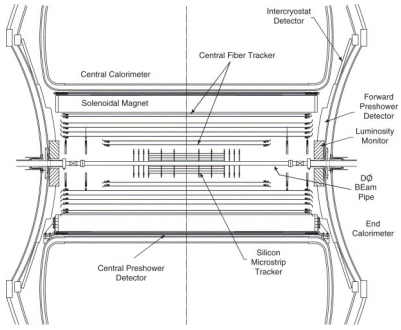

(b) Cross section of the center region of the D0 detector[5].

Figure 3.1: Detector Diagrams. These diagrams focus on the center region of the detector; from the beam tube out to the calorimeter.

	Integrated Luminosity (pb^{-1})
RunIIa	1081.21
RunIIb1	1217.67
RunIIb2	3039.84
RunIIb3	1994.27
Total	**7332.99**

Table 1: Integrated Luminosity Values for the Different Run Periods. Here are the luminosity values for the run periods used in this analysis; namely Run2a, Run2b1, Run2b2, and Run2b3. Integrated luminosity is representative of the amount of data collected by the detector.

Detector upgrades occurred between RunIIa and RunIIb. The differences in the detector have been taken into account in our photon event selection process. Integrated luminosity values recorded in the different run periods are listed in Table 1. Luminosity is a measurement of the number of particles per unit area per unit time. When this value is integrated over the amount of time collisions were occurring, we have an integrated luminosity value. Therefore, integrated luminosity can be thought of as a measurement of the amount of data collected during a specified amount of time. It has the unit of inverse-barn (the unit of barns is discussed in more detail in Section 12). For the Tevatron, integrated luminosity is on the order of inverse-femtobarn and has an uncertainty of 6.1% [3].

4 Photon Identification

As discussed in Section 3, it is necessary to have a method of identifying which particles, in a reconstructed cluster of energy in the EM calorimeter, are photons. Photon requirements include: [6]

1. A minimum of 90% of the energy of the cluster be deposited in the EM calorimeter. Since photons are solely EM objects, they lose most of their energy in the EM section of the calorimeter.
2. The calorimeter isolation variable must be less than 0.07. If the amount of total energy deposited in the calorimeter in a cone of radius 0.4 is E_{tot} and the amount of EM energy deposited in the calorimeter in a cone of radius 0.2 is E_{em}, then $\frac{E_{tot}-E_{em}}{E_{em}}$ must be less than 0.07. The radius of a cone is defined as $R = \sqrt{(\Delta\eta)^2 + (\Delta\phi)^2}$, where η is the pseudo-rapidity ($\eta = -\ln(\tan(\frac{\theta}{2}))$ where θ is the polar angle), and ϕ is the azimuthal angle. This is saying that the energy around a photon should be minimal; the photon is isolated.
3. The track isolation variable must be less than 2 GeV. This variable is defined as the scalar sum of transverse momenta of charged particles that have an origin at the interaction vertex in an annulus with a radius between 0.05 and 0.4. Therefore, this is another way of ensuring the photon is isolated.
4. The photon must be detected in the central section of the calorimeter. This is done for accuracy reasons.
5. The shower shape must be consistent with that of a photon.
6. There must not be a track in the central tracking system, or too may hits in the silicon microstrip tracker and scintillating fiber tracker. These systems detect charged particles. Because photons are neutral, they are not expected to cause hits in the tracking detector.
7. There must be energy deposits in the central preshower detector that match up with the rest of the shower.

Part II
Data Analysis

5 Photon Selection

A data sample (called a photon sample) was made with some of the following requirements: [6]

1. A single photon with a transverse momentum larger than 90 GeV.
2. A minimum of one reconstructed interaction vertex (see Section 6) with MET larger than 70 GeV. The interaction vertex must coincide with the direction of the photon.
3. No jets with a transverse momentum larger than 15 GeV. This allows us to avoid large MET values due to incorrectly measured jet energy.
4. Events must not have a reconstructed muon.
5. There be no isolated tracks with transverse momentum greater than 6.5 GeV. This ensures that there are fewer misidentified photons by excluding leptons that have left a track in the tracker, but are not reconstructed in other areas of the detector.

6 EM Pointing Algorithm

The electromagnetic (EM) pointing algorithm is used to help identify events in the detector as photons or as background events. The EM pointing algorithm uses information from the central preshower detector and the electromagnetic calorimeter to determine where an EM shower originated and where it pointed (see Figure 6.1). Using the EM pointing algorithm in the r-z direction we can estimate the z-coordinate of the interaction vertex. Looking at the r-φ direction we can calculate the distance of closest approach (see Section 7), a variable that is very helpful in data restriction and background analysis.

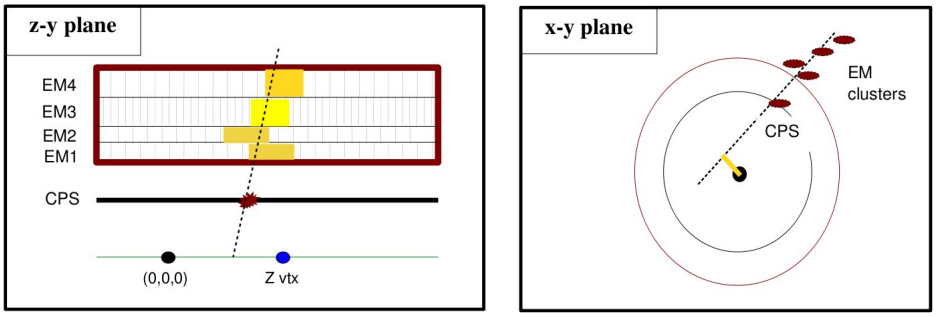

(a) r-z plane (beam horizontal direction) [3]

(b) r-φ plane (beam in/out of page) [3]

Figure 6.1: EM Pointing Algorithm.

7 DCA histograms

The distance of closest approach (DCA) is the distance between the projected interaction vertex, calculated using the EM pointing algorithm, and the actual interaction vertex. Figure 6.1b is a visual representation on how a DCA value is calculated. The EM pointing algorithm uses data (red dots) from the EM calorimeter and the central preshower detector to determine a projected path of the photon (dotted line). The DCA is the perpendicular distance between the photon trajectory and the actual interaction vertex (yellow line). This DCA value is used to limit our data sample; our data sample is limited to events that have a DCA value less than 4 centimeters. DCA is also used to estimate the number of non-collision and misidentified jets background present in our analysis (see Section 8) [6]. See Figure 7 for DCA plots of RunIIa, RunIIb1, RunIIb2, and RunIIb3.

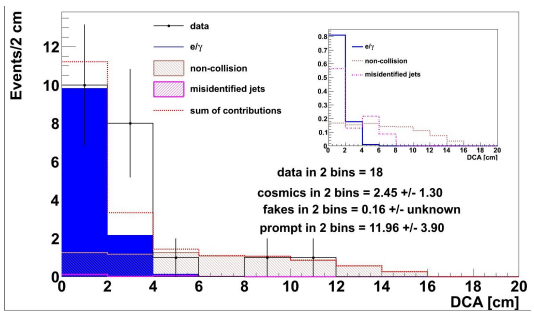

(a) RunIIa

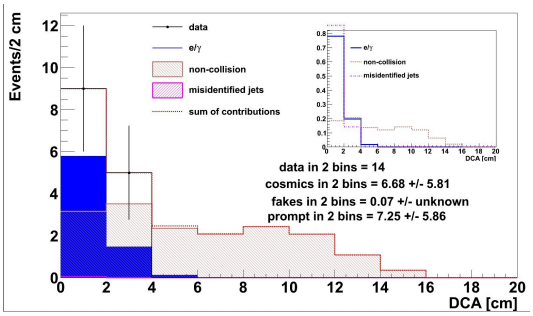

(b) RunIIb1

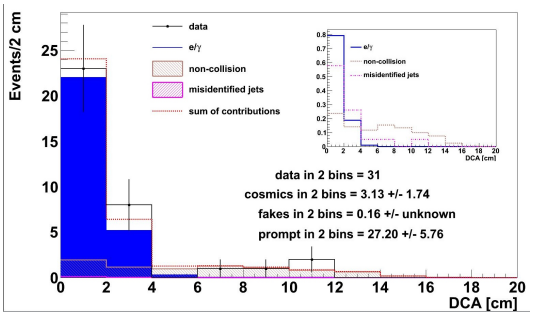

(c) RunIIb2

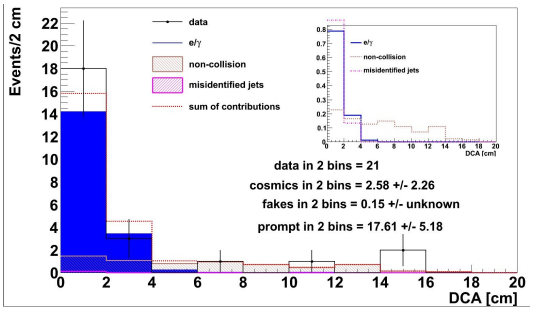

(d) RunIIb3

Figure 7.1: DCA Histograms.

Part III
Background Analysis

8 Non-collision and Misidentified jets

These backgrounds are extrapolated from the DCA histograms. When the EM pointing algorithm is used on a misidentified jet, it is more likely to point back to a spot further away from the interaction vertex than a photon would. This is because the EM clusters for a jet will not be very well localized. Therefore, misidentified jets can have a high DCA value. Non-collision events have a larger DCA value still, because these particles do not originate from the detector, so they are even less likely to point back to the interaction vertex [6]. The DCA histogram is run though a fitter program to determine how many non-collision events and misidentified jets are present in the data sample.

The backgrounds estimated from the DCA fitter program need to be properly scaled. This is done by calculating the number of jets that have been misidentified as photons. To calculate the number of misidentified jets, two different data samples were analyzed: a fake photon sample, and an EM plus jet sample. The fake photon sample consists of events which have the same requirements as the photon sample listed in Section 5, except that the photon track isolation value is inverted. This allows for the fake photon sample to be flooded with misidentified jets. On the other hand, the EM plus jet sample is made by requiring all the same photon identification requirements listed in Section 4 except for the track isolation requirement. Because tracks are not required to be isolated, both jets and EM objects are present in the sample. Next, using the EM plus jet sample, we determined the number of events that passed track isolation (N_1) and the number of events that failed track isolation (N_2). The number of misidentified jets is equal to N_1/N_2 multiplied by the number of events in the fake photon sample. This value allows us to correctly scale the templates used in fitter program [6].

Note: The calculation of a jet scale factor was more cumbersome than expected. Due to time restrictions, a scale factor value was not explicitly calculated in this analysis. A

scale factor value of 0.01 was used [3]. This value is consistent with the results of a previous analysis, which used the same scale factor calculation process.

9 Z plus Gamma

A physics background in our analysis is $Z + \gamma \rightarrow \nu\overline{\nu} + \gamma$ in which the resultant photon is detected, but not the neutrinos. This background is unavoidable and produces the same signature as the $p+\bar{p} \rightarrow \gamma+G_{KK}+X$ because the neutrinos produced in the Z decay manifest as missing transverse energy. Therefore, this event is misidentified as a single photon event with MET. The contribution of this background was calculated through Monte Carlo (MC) event generations. A MC event generation is a set of random simulated data values made for a specified reaction [3].

10 $W \rightarrow e\nu$ and $W + \gamma$

A non-physics background, which arises from the instrumentation, is $W \rightarrow e\nu$. Here, an electron is misidentified as a photon. This background is estimated through the analysis of an electron sample. The same requirements are applied to this electron sample as on the photon sample (see Section 5). The number of events that pass are then scaled by $(1-\epsilon)/\epsilon$ where epsilon is the track reconstruction efficiency, which has a value of (98.6 ± 0.1) percent [6].

Another non-physics background is the $W + \gamma$ interaction, which also arises from the instrumentation. In this reaction, the charged lepton produced in the W decay is left undetected. We find the background contribution of this reaction through Monte Carlo generations and analysis [6].

Note: The $W \rightarrow e\nu$ and $W + \gamma$ background have temporarily been omitted from this analysis because of time constraints. Both these backgrounds are small compared to the

	RunIIa	RunIIb1	RunIIb2	RunIIb3
Non-Collision	2.45 ± 1.30	6.68 ± 5.81	3.13 ± 1.74	2.58 ± 2.26
Misidentified Jets	0.160 ± 0.080	0.070 ± 0.035	0.160 ± 0.080	0.15 ± 0.075
Z + γ	13.84 ± 1.31	11.78 ± 1.13	23.81 ± 2.25	11.98 ± 1.14
Data	18	14	31	21
Total Background	**16.45 ± 1.85**	**18.53 ± 5.92**	**27.10 ± 2.84**	**14.71 ± 2.53**

Table 2: Background Summary Table. Listed are the different backgrounds for each of the different run periods used in this analysis. Also listed is the number of data.

$Z + \gamma$ background, so time was spent focusing on this background in detail. A summary of the background values used in our analysis is listed in Table 2.

Part IV
Limit Value Calculations

11 Signal sample

A signal sample is used to analyze what we expect to see in our data. Our signal sample includes events that simulate $p + \bar{p} \rightarrow \gamma + G_{KK} + X$. A signal sample was generated for 2 to 8 extra dimensions using a fixed value of M_D = 1500 GeV. The signal sample is used to calculate acceptance and helps determine limits on the cross section. The acceptance is the final number of signal events that pass through our analysis divided by the total number of signal events generated. Tabulated acceptance values are listed in Table 3.

12 Cross Section Limits

The cross section of a specific interaction is a way of expressing the likelihood of the specified interaction to occur. It has the units of barns (b). A barn is a unit of area. One barn is equal to 10^{-28} m^2. Cross section $\{\sigma\}$ is dependent on the integrated luminosity $\{\mathscr{L}\}$, the acceptance $\{\alpha\}$ and the number of events $\{N\}$. Specifically,

n	RunIIa	RunIIb1	RunIIb2	RunIIb3
2	0.175 ± 0.007	0.135 ± 0.007	0.116 ± 0.013	0.099 ± 0.007
3	0.170 ± 0.004	0.13 ± 0.003	0.110 ± 0.014	0.097 ± 0.008
4	0.166 ± 0.002	0.123 ± 0.002	0.112 ± 0.016	0.095 ± 0.007
5	0.170 ± 0.001	0.122 ± 0.001	0.105± 0.013	0.091 ± 0.010
6	0.158 ± 0.001	0.117 ± 0.001	0.102 ± 0.015	0.089 ± 0.006
7	0.168 ± 0.000	0.113 ± 0.001	0.102 ± 0.012	0.089 ± 0.007
8	0.147 ± 0.000	0.111 ± 0.000	0.097 ± 0.012	0.083 ± 0.007

Table 3: Acceptance Values. Acceptance is the final number of signal events that pass through our analysis divided by the total number of signal events generated.

$$\sigma = \frac{N}{\mathscr{L}\alpha} \tag{12.1}$$

The particle collision at the Tevatron that we are looking at has a very small cross sectional value, on the order of picobarns (pb). Cross section limit values were calculated using an executable available through the D0 code repository. This uses the modified frequentist approach, which is based off a log-likelihood ratio test statistic [6]. The cross section limit is dependent on the number of events that pass through our analysis, the number of background events and its uncertainty, the acceptance value for a specific number of dimensions and its uncertainty, and the luminosity value for a specific Run period and its error.

13 M_D Limit Values

According to ADD model, the fundamental Planck scale and the cross section are related in the following way,

$$M_D^{2+n} = \frac{1}{\sigma_{limit}}(\sigma_{M_{Dfixed}} M_{D_{fixed}}^{2+n}) \tag{13.1}$$

where $M_{D_{fixed}}$ is the value of 1500 GeV that we set in our signal sample (see Section 11), and σ_{limit} are the values listed in Table 4.

From this relation, lower limits were calculated for M_D with 95% confidence level using

n	RunIIa (pb)	RunIIb1 (pb)	RunIIb2 (pb)	RunIIb3 (pb)
2	0.0540	0.0668	0.0448	0.0786
3	0.0554	0.0696	0.0476	0.0804
4	0.0564	0.0730	0.0478	0.0818
5	0.0554	0.0735	0.0495	0.0879
6	0.0594	0.0769	0.0523	0.0866
7	0.0558	0.0795	0.0513	0.0883
8	0.0638	0.0812	0.0539	0.0939

(a) Observed Cross Section Limit

n	RunIIa (pb)	RunIIb1 (pb)	RunIIb2 (pb)	RunIIb3 (pb)
2	0.0443	0.0847	0.0341	0.0434
3	0.0455	0.0881	0.0363	0.0442
4	0.0464	0.0925	0.0363	0.0450
5	0.0455	0.0932	0.0377	0.0481
6	0.0489	0.0973	0.0398	0.0477
7	0.0458	0.1007	0.0391	0.0486
8	0.0524	0.1028	0.0410	0.0517

(b) Expected Cross Section Limit

Table 4: Cross Section Limit Values

7.3 fb^{-1} of data. The 'observed' limit is the value calculated when analyzing the observed data, while the 'expected' limit is the value calculated as if the observed matched the background. The results are listed in Table 5.

Part V
Conclusions

We have analyzed 7.3 fb^{-1} of data from the D0 detector and have calculated lower limits on the fundamental Planck scale of 1026, 966, 932, 910, 892, 882, 868 GeV for 2, 3, 4, 5, 6, 7, and 8 number of extra dimensions respectively. This is plotted in Figure 13.1 and Figure 13.2. The plot in Figure 13.2 compares this analysis to a previous analysis using 2.7 fb^{-1}. The addition of more data has improved the limit values. We can see that the observed and expected values show reasonable agreement and are within one standard deviation of the

n	Observed (Expected) Lower Limits (GeV)
2	1026 (1083)
3	966 (1008)
4	932 (966)
5	910 (938)
6	892 (916)
7	882 (903)
8	868 (886)

(a) Current Analysis, 7.3 fb^{-1}

n	Observed (Expected) Lower Limits (GeV)
2	970 (1037)
3	899 (957)
4	867 (916)
5	848 (883)
6	831 (850)
7	834 (841)
8	804 (816)

(b) Previous Analysis, 2.7 fb^{-1}

Table 5: Lower Limit Values for M_D

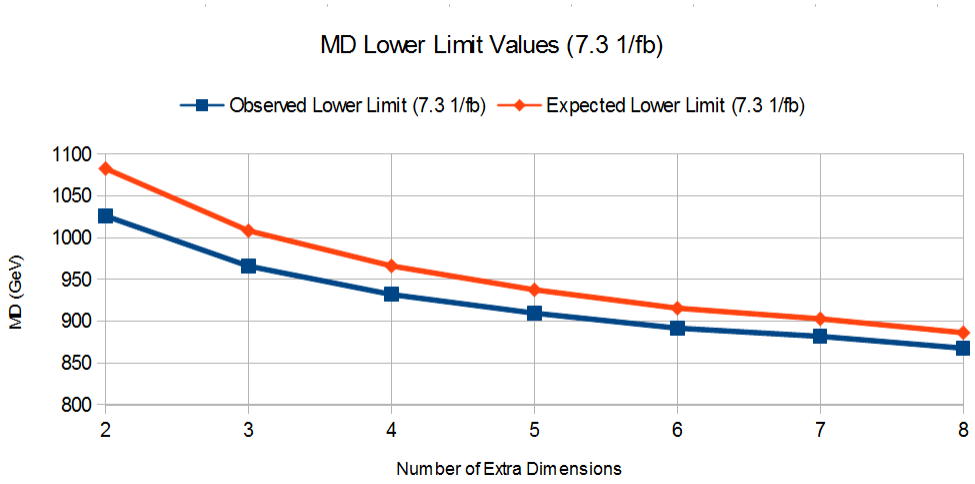

Figure 13.1: Lower Limit Values for M_D

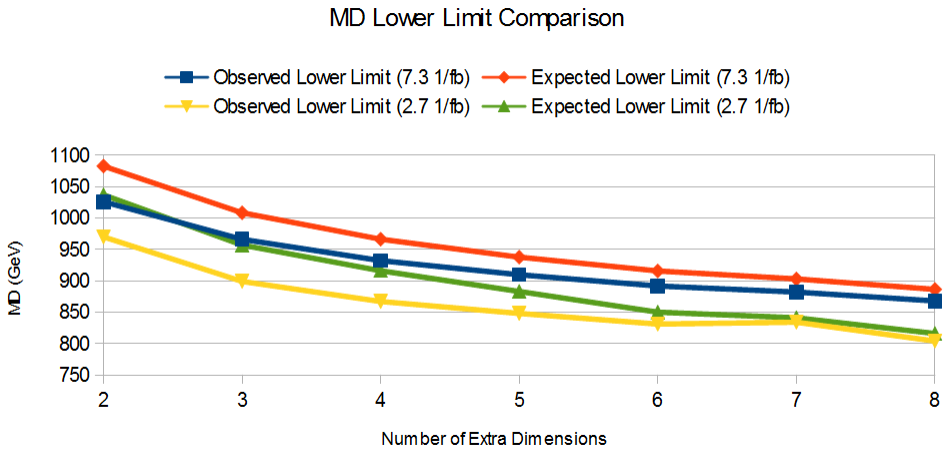

Figure 13.2: Lower Limit Value Plot for M_D

mean. Therefore, we see no evidence for the existence of large extra dimensions.

Nomenclature

ADD Arkani-Hamad, Dimopoulos, Dvali

b barn

CPS Central Preshower System

DCA Distance of Closest Approach

EM Electromagnetic

LED Large Extra Dimension

MC Monte Carlo

MD Fundamental Planck Scale

MET Missing Transverse Energy

References

[1] Arkani-Hamad, Nima, Savas Dimopoulos, and Gia Dvali. "The Hierarchy Problem and New Dimensions at a Millimeter." *Physics Letters* B 429(1998): 263-72. Print.

[2] "Accelerator - Fermilab's Tevatron." Fermilab. Fermi National Accelerator Laboratory, 02 Dec. 2011. Web. 10 Apr. 2013. <http://www.fnal.gov/pub/science/accelerator/>.

[3] Carrera, Edgar. "Search for Large Extra Dimensions via Single Photon plus Missing Energy Final States at $\sqrt{s} = 1.96$TeV." Thesis. Florida State University, 2009. Print.

[4] DZero Calorimeter Diagram. Digital image. Fermilab. Fermi National Accelerator Laboratory, n.d. Web. 10 Apr. 2013. <http://www-d0.fnal.gov/Run2Physics/WWW/drawings/run2_nim/calorimeter-color.gif>.

[5] DZero Collaboration. "The Upgraded D0 Detector." Nuclear Instruments and Methods in Physics Research Section A: Accelerators, Spectrometers, Detectors and Associated Equipment 565.2 (2006): 463-537. ScienceDirect. Web. 10 Apr. 2013. <http://www.sciencedirect.com/science/article/pii/S0168900206010357>.

[6] DZero collaboration. "Search for Large Extra Dimensions via Single Photon plus Missing Energy Final States at $\sqrt{s} = 1.96$ TeV." *Physical Review Letters* 101(2008): 011601.1-011601.7. Print.